Chemical Science

ROYAL SOCIETY OF CHEMISTRY

EDGE ARTICLE

View Article Online
View Journal | View Issue

Open Access Article. Published on 28 September 2023. Downloaded on 10/30/2025 1:26:33 AM.
This article is licensed under a Creative Commons Attribution-NonCommercial 3.0 Unported Licence.

Check for updates

Cite this: *Chem. Sci.*, 2023, **14**, 11261

All publication charges for this article have been paid for by the Royal Society of Chemistry

Calculation-assisted regioselective functionalization of the imidazo[1,2-*a*]pyrazine scaffold *via* zinc and magnesium organometallic intermediates†

Agonist Kastrati, ‡[a] Alexander Kremsmair,‡[a] Alisa S. Sunagatullina,[a] Vasilii Korotenko,[a] Yusuf C. Guersoy,[a] Saroj K. Rout,[a] Fabio Lima,[b] Cara E. Brocklehurst,[b] Konstantin Karaghiosoff,[a] Hendrik Zipse *[a] and Paul Knochel *[a]

Received 6th June 2023
Accepted 24th September 2023

DOI: 10.1039/d3sc02893c

rsc.li/chemical-science

Straightforward calculations such as determinations of pK_a values and N-basicities have allowed the development of a set of organometallic reactions for the regioselective functionalization of the underexplored fused N-heterocycle imidazo[1,2-*a*]pyrazine. Thus, regioselective metalations of 6-chloroimidazo[1,2-*a*]pyrazine using TMP-bases (TMP = 2,2,6,6-tetramethylpiperidyl) such as TMPMgCl·LiCl and $TMP_2Zn\cdot 2MgCl_2\cdot 2LiCl$ provided Zn- and Mg-intermediates, that after quenching with various electrophiles gave access to polyfunctionalized imidazopyrazine heterocycles. Additionally, the use of $TMP_2Zn\cdot 2MgCl_2\cdot 2LiCl$ as base for the first metalation allowed an alternative regioselective metalation. Nucleophilic additions at position 8 as well as selective Negishi cross-couplings complete the set of methods for selectively decorating this heterocycle of the future.

Introduction

N-heterocycles are ubiquitous scaffolds in pharmaceutical and agrochemical research.[1] They possess unique physicochemical and medicinal properties in addition to favorable pharmacokinetics, which make their efficient further functionalization an attractive research goal.[2] Besides standard N-heterocycles such as pyridines, diazines and indoles for which functionalization methods are well established, there is a current trend to investigate less common N-heterocycles as pharmaceutical scaffolds.[3] Recently, we have reported the decoration of a range of new fused N-heterocycles such as pyrazolo[1,5-*a*]pyrimidines (**1**) and imidazo[1,2-*b*]pyridazines (**2**).[4] From these studies, we were anticipating useful properties of the imidazo[1,2-*a*]pyrazine ring system (**3**, Scheme 1a). This structural motif has already found pharmaceutical applications as the kinase inhibitor **4**[5] and the AKT inhibitor **5**[6] (Scheme 1a).[7] However, most previous synthetic approaches towards the functionalization of the imidazo[1,2-*a*]pyrazine scaffold involve either electrophilic bromination,[8] followed by Suzuki–Miyaura cross-couplings, or transition metal-catalyzed direct C–H arylations.[9] As a result, there are significant limitations in scope for preparing more complex and multifunctionalized derivatives. Combining theoretical calculations and extensive experimental knowledge in the functionalization of N-heterocycles has now allowed us to develop a rational approach towards the decoration of this relatively underexplored heterocyclic scaffold. Thus, we calculated the pK_a values of all ring hydrogens of **3**[4a,b] in order to predict the metalation regioselectivity with TMP-bases (TMP = 2,2,6,6-tetramethylpiperidyl).[10] We have found very similar pK_a values of position 3 and 5 as well as prohibitively high values for metalations in position 6 and 8 for the unsubstituted scaffold **3**. In fact, metalation of **3** with TMPMgCl·LiCl (**11**) in THF (−60 °C, 0.5 h) produced after deuterolysis quench a 60 : 40 mixture of C3/C5 deuterated products.[11] This data let us consider the introduction of an electronegative substituent, which would lower all the pK_a values and introduce a larger pK_a difference between positions 3 and 5. A chlorine substituent at position 6 was an ideal solution to these problems since it can be readily removed or substituted.[12] A web-search showed that 6-chloroimidazo[1,2-*a*]pyrazine (**6**) is easily prepared[13] and commercially available. Calculations of the pK_a values of **6** confirmed our hypothesis (Scheme 1b). Furthermore, thanks to extensive calculations, we were able to get a deeper and more accurate insight into the metalation regioselectivities of various

[a]*Department Chemie, Ludwig-Maximilians-Universität München, Butenandtstrasse 5-13, Haus F, 81377 München, Germany. E-mail: zipse@cup.uni-muenchen.de; knoch@cup.uni-muenchen.de*

[b]*Global Discovery Chemistry, Novartis Institutes for BioMedical Research, 4057 Basel, Switzerland*

† Electronic supplementary information (ESI) available. CCDC 2258909–2258912. For ESI and crystallographic data in CIF or other electronic format see DOI: https://doi.org/10.1039/d3sc02893c

‡ These authors contributed equally.

Open Access Article. Published on 28 September 2023. Downloaded on 10/30/2025 1:26:33 AM.
This article is licensed under a Creative Commons Attribution-NonCommercial 3.0 Unported Licence.

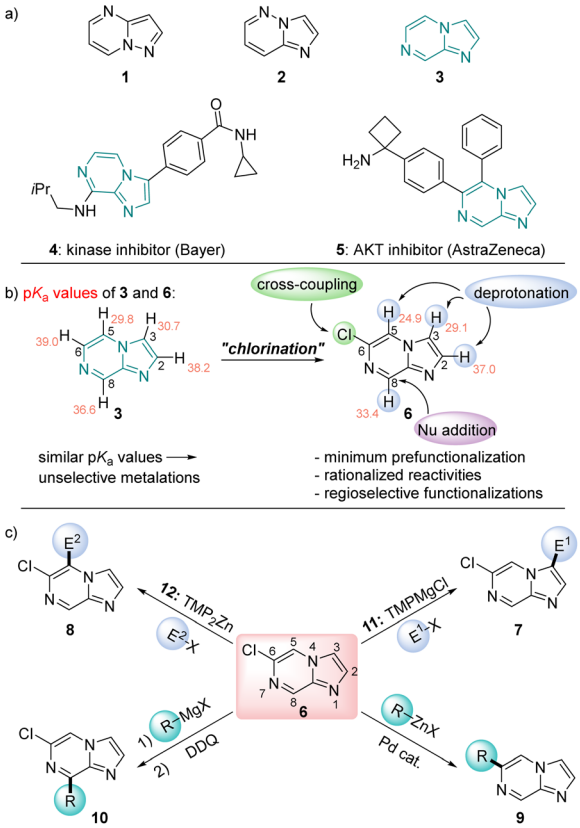

Scheme 1 (a) Heterocycles of the future **1**, **2** and **3**.[3] (b) Calculated pK_a values indicated that a chlorination led to enhanced pK_a differences. (c) Reactivity pattern of **6** producing imidazo[1,2-*a*]pyrazines of type **7**–**10**. Salts are omitted for clarity.

substituted imidazo[1,2-*a*]pyrazines of type **6**. We realized that the relative energies of the organometallic intermediates and the inclusion of additives such as LiCl in the calculations provided a basis for the rationalization of observed regioselectivities.

Herein, we report a versatile selective functionalization of this scaffold using regioselective metalations, nucleophilic additions and cross-couplings. As bases we have used TMP-bases[10] of Mg[14] and Zn[15] such as TMPMgCl·LiCl[14a] (**11**), and $TMP_2Zn\cdot 2MgCl_2\cdot 2LiCl$[15a] (**12**, Scheme 1c).[16]

Results and discussion

Thus, we have found that the metalation of 6-chloroimidazo[1,2-*a*]pyrazine (**6**) with TMPMgCl·LiCl (**11**) in THF led to a selective magnesiation at position 3 at −60 °C within 30 min affording magnesium derivatives of type **13**.[17] The quenching of **13** with various electrophiles gave 3,6-disubstituted imidazo[1,2-*a*]pyrazines **7a–g** in 40–78% yield (Scheme 2).[18] Iodolysis of **13** gave the corresponding iodide **7a** in 78% yield. Whereas, treatment of **13** with allyl bromide or acyl chlorides (25 °C, 2 h) in the presence of catalytic amounts of CuCN·2LiCl[19] (20–50 mol%) furnished allylated derivative **7b** in 56% yield and ketones **7c** and **7d** in 40–56% yield. The scope was further increased by treating Mg-intermediate **13** with commercially

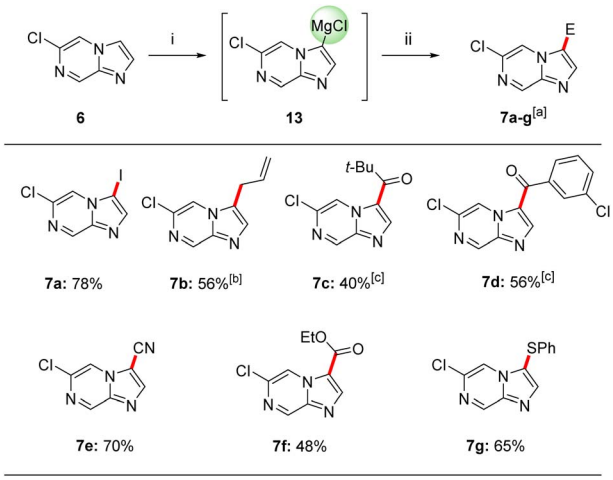

Scheme 2 Regioselective magnesiation of 6-chloroimidazo[1,2-*a*]pyrazine (**6**) using TMPMgCl·LiCl (**11**) followed by quenching with electrophiles. Reagents and conditions: (i) TMPMgCl·LiCl (**11**, 1.2 equiv.), THF, −60 °C, 30 min; (ii) E-X, THF, 25 °C, 0.15–2 h; [a]isolated yield of analytically pure products; [b]the allylation was mediated by CuCN·2LiCl (50 mol%), THF, 25 °C, 1.5 h; [c]the acylation was mediated by CuCN·2LiCl (20–50 mol%), THF, 25 °C, 2 h.

available TsCN, ethyl cyanoformate or freshly prepared $PhSO_2$-SMe[20] affording cyano-derivative **7e**, ester derivative **7f** and thioether **7g** in 48–70% yield. The structure of **7a** was confirmed by single crystal X-ray diffraction.[11] DFT calculations confirmed the observed metalation regioselectivity at position 3 and clearly showed that the intermediate **13** was the most stable organometallic intermediate. In addition, we found that the NBO

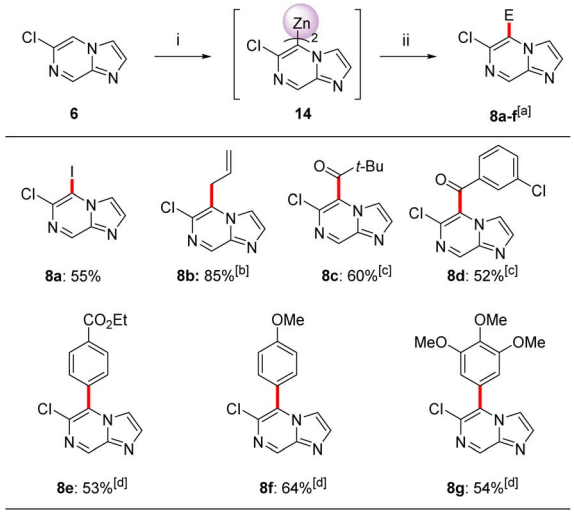

Scheme 3 Regioselective zincation of 6-chloroimidazo[1,2-*a*]pyrazine (**6**) using $TMP_2Zn\cdot 2MgCl_2\cdot 2LiCl$ (**12**) followed by quenching with electrophiles. Reagents and conditions: (i) $TMP_2Zn\cdot 2MgCl_2\cdot 2LiCl$ (**12**, 0.6 equiv), THF, −20 °C, 15 min; (ii) E-X, THF, 25 °C, 2 h. [a]Isolated yield of analytically pure products; [b]the allylation was mediated by CuCN·2LiCl (20 mol%), THF, 25 °C, 1.5 h; [c]the acylation was mediated by CuCN·2LiCl (20 mol%), THF, 25 °C, 2 h. [d]$Pd(PPh_3)_4$ (5 mol%), THF, 50 °C, 2 h.

 © 2023 The Author(s). Published by the Royal Society of Chemistry

Open Access Article. Published on 28 September 2023. Downloaded on 10/30/2025 1:26:33 AM.
This article is licensed under a Creative Commons Attribution-NonCommercial 3.0 Unported Licence.

Scheme 4 Thermodynamically driven regioselectivity switch in the metalation of 6-chloroimidazo[1,2-*a*]pyrazine using either TMPMgCl·LiCl (**11**) or $TMP_2Zn·2MgCl_2·2LiCl$ (**12**). Salts are omitted for clarity.

charge at C3 was the most negative among all carbon atoms in heterocycle **6**.[11]

Interestingly, the treatment of 6-chloroimidazo[1,2-*a*]pyrazine (**6**) with $TMP_2Zn·2MgCl_2·2LiCl$ (**12**) in THF led to a complete regioselectivity switch affording diheteroarylzinc derivatives of type **14** within 15 min at −20 °C.[17] Subjecting this intermediate to various electrophiles gave 5,6-disubstituted imidazo[1,2-*a*]pyrazine **8a–g** in 52–85% isolated yield (Scheme 3).

Thus, iodolysis of **14** gave the corresponding iodide **8a** in 55% yield. Whereas, treatment of **14** with CuCN·2LiCl (20 mol%) followed by addition of allyl bromide or different acyl chlorides (25 °C, 1.5–2 h) furnished the allylated derivative **8b** in 85% yield and ketones **8c** and **8d** in 52–60%. Negishi cross-couplings[21] of the diheteroarylzinc derivative **14** with aryl iodides in the presence of catalytic amounts of $Pd(PPh_3)_4$ (5 mol%, 50 °C, 2 h) gave the arylated N-heterocycles **8e–8g** in 53–64% isolated yield. The structure of **8b** was confirmed by single crystal X-ray diffraction.[11]

The rationalization of these complementary regioselectivites may be tentatively done based on relative basicities. Thus, DFT calculations indicated that the C5-metalated intermediate **14** was preferred for thermochemical reasons, possibly due to attractive intramolecular CH···Cl interactions.[11] The Zn-base **12** (bearing a N–Zn bond) is less reactive than the Mg-base **11** which is bearing a more ionic N–Mg bond. The temperatures −60 °C in the case of **13** and −20 °C in the case of **1** have been optimized to achieve the best yields.[22] The observed regioselectivity reflects according to our calculations the relative stability of the produced organometallic intermediates **13** or **14** and overcomes complex-inducing proximity effects (Scheme 4).[23]

A second zincation of 3,6-disubstituted imidazo[1,2-*a*]pyrazine (**7e**) using $TMP_2Zn·2MgCl_2·2LiCl$ (**12**) was also possible (Scheme 5). Thus, treatment of imidazo[1,2-*a*]pyrazine-3-carbonitrile (**7e**) with **12** (0.6 equiv., THF, −20 °C, 15 min) provided diheteroarylzinc intermediate **15**, which was successfully quenched with electrophiles providing trisubstituted imidazo[1,2-*a*]pyrazines **16a–e** in 33–72% yield. Thus, iodolysis of **15** afforded iodide **16a** in 52% yield. Whereas, treatment of **15** with CuCN·2LiCl (20 mol%) followed by addition of allyl bromide or pivaloyl chloride (25 °C, 2 h) furnished allyl derivative **16b** in 50% yield and ketone **16c** in 33% yield. Negishi cross-couplings of the diheteroarylzinc derivative **15** with aryl iodides in the presence of catalytic amounts of $Pd(PPh_3)_4$ (5 mol%, 50 °C, 2 h) gave the arylated N-heterocycles **16d–e** in

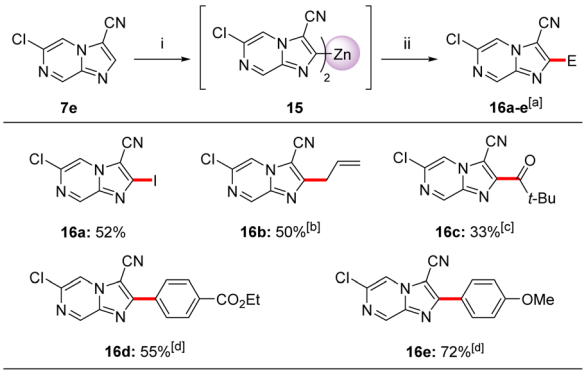

Scheme 5 Selective zincation of N-heterocycle **7e** using $TMP_2Zn·2MgCl_2·2LiCl$ (**12**) followed by quenching with electrophiles affording trisubstituted N-heterocycles **16a–e**. Reagents and conditions: (i) $TMP_2Zn·2MgCl_2·2LiCl$ (**12**, 0.55 equiv.), THF, −20 °C, 15 min; (ii) E-X, THF, 25 °C, 2 h. [a]Isolated yield of analytically pure products; [b]the allylation was mediated by CuCN·2LiCl (20 mol%), THF, 25 °C, 1.5 h; [c]the acylation was mediated by CuCN·2LiCl (20 mol%), THF, 25 °C, 2 h; [d]$Pd(PPh_3)_4$ (5 mol%), THF, 50 °C, 2 h.

55–72% yield. The metalation regioselectivity at position 2 of **7e** was investigated by DFT calculations showing that C2 metalated intermediate **15** was stabilized by the neighbouring LiCl and $MgCl_2$ *via* non-covalent interactions. In this case, we have also considered an equilibrium between various Zn-TMP bases which may contain TMP_2Zn as well as TMPZnCl. In addition, we have found that the cyano group was responsible for unfavourable steric effects onto the C5 position.[11]

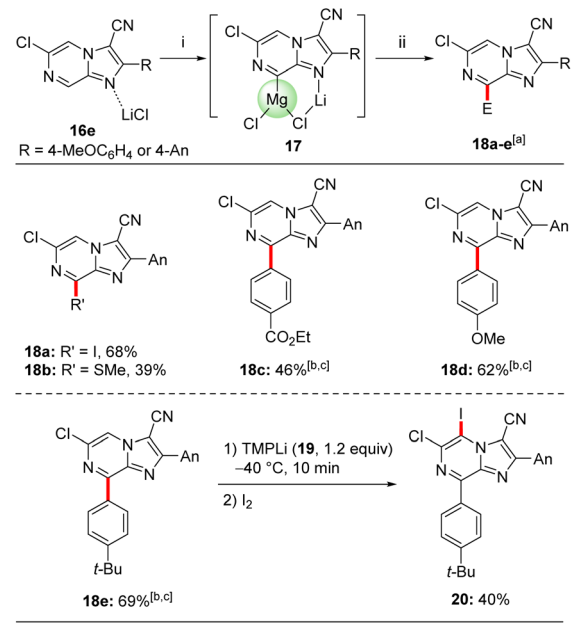

Scheme 6 Magnesiation of the trisubstituted imidazopyrazine **16e** using TMPMgCl·LiCl (**11**) followed by various quenching reactions with electrophiles. Reagents and conditions: (i) TMPMgCl·LiCl (**11**, 1.2 equiv.), THF, −40 °C, 30 min; (ii) E-X, THF, 25 °C, 0.15–2 h. [a]Isolated yield of analytically pure products; [b]transmetalation with $ZnCl_2$ (1 M solution in THF, 1.2 equiv.), 15 min. [c]$Pd(PPh_3)_4$ (5 mol%) THF, 50 °C, 2 h.

Open Access Article. Published on 28 September 2023. Downloaded on 10/30/2025 1:26:33 AM.
This article is licensed under a Creative Commons Attribution-NonCommercial 3.0 Unported Licence.

A further magnesiation of 2,3-disubstituted 6-chloroimidazo[1,2-*a*]pyrazine derivative **16e** was possible (Scheme 6). Thus, treating the trisubstituted heterocycle **16e** with TMPMgCl·LiCl (**11**) in THF at −40 °C within 30 min afforded the magnesiated species **17**. This regioselectivity can be rationalized with calculations including LiCl, which formed the very stable mixed Li,Mg-intermediate **17** depicted in Scheme 6.[11] Its quenching with electrophiles gave access to tetrasubstituted derivatives **18a–e** in 39–69% yield. Thus, iodolysis of **17** provided the iodide **18a** in 68% yield. Treatment of **17** with $PhSO_2SMe$ afforded the desired sulfide **18b** in 39% yield. After transmetalation with a solution of $ZnCl_2$ (1 M in THF, 1.2 equiv.) for 15 min the resulting heteroarylzinc species was subjected to Negishi cross-couplings with aryl iodides in the presence of catalytic amounts of $Pd(PPh_3)_4$ (5 mol%, THF, 50 °C, 2 h) giving the arylated N-heterocycles **18c–e** in 46–69% yield. The structure of **18a** was confirmed by single crystal X-ray diffraction.[11]

Lithiation of the trisubstituted N-heterocycle **18e** using TMPLi (**19**, 1.2 equiv.) at −40 °C, 10 min led to a regioselective lithiation at position 5 and subsequent trapping with iodine gave the fully functionalized N-heterocycle **20** in 40% yield (Scheme 6).[24] The presence of chlorine- and iodine-substituents now opens the way for diverse further functionalizations. Concerning the replacement of the chlorine substituent, this was demonstrated by submitting 6-chloroimidazo[1,2-*a*]pyrazine (**6**) to cross-couplings with functionalized organozinc reagents of type **21**[25] in the presence of 5 mol% of Pd-PEPPSI-iPr[26] or Pd-PEPPSI-iPent[27] affording functionalized 6-substituted imidazo[1,2-*a*]pyrazines **22a–e** in up to 98% yield (Scheme 7). Thus, cross-coupling of **6** with arylzinc reagents **21a** or **21b** bearing a sensitive ester[25c] or cyano[25a] functionality led to 6-arylated imidazo[1,2-*a*]pyrazines **22a-b** in 90–93% yield. Interestingly, alkylzinc reagents such as **21c**[25d] or **21d**[25d] showed superior results when the more sterically hindered catalyst Pd-PEPPSI-iPent (5 mol%)[27] was used resulting in the N-heterocycles **22c–d** in up to 98% yield. Finally, functionalized benzylic zinc reagent **21e**[25b] was an excellent substrate for this cross-coupling leading to the benzoylated heterocycle **22e** in 95% yield. Related Suzuki–Miyaura cross-couplings can be performed using **7e** and arylboronic acid esters in the presence of $Pd(PPh_3)_4$ (10 mol%), albeit in lower yields (up to 50% isolated yield) and under harsher reaction conditions (100 °C, 5 h).[11]

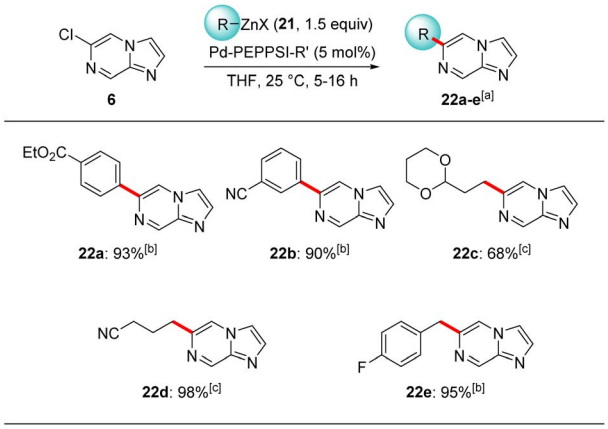

Scheme 7 Palladium-catalyzed Negishi cross-couplings of **6** using functionalized aryl, alkyl and benzylic zinc reagents of type **21** leading to functionalized 6-substituted imidazo[1,2-*a*]pyrazines **22a–e**. Reagents and conditions: X = Cl·MgICl·LiCl, Cl·MgBrCl·LiCl or Cl·$MgCl_2$·LiCl; R = Alk, Ar, Bz; R′ = iPr or iPent. [a]Isolated yield of analytically pure products; [b]the cross-coupling was catalyzed by Pd-PEPPSI-iPr (5 mol%), THF, 25 °C, 5 h; [c]the cross-coupling was catalyzed by Pd-PEPPSI-iPent (5 mol%), THF, 25 °C, 16 h.

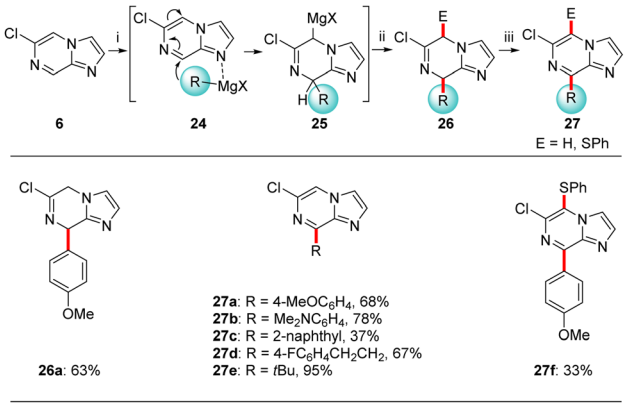

Scheme 8 Nucleophilic addition of Grignard reagents of type **23** to 6-chloroimidazo[1,2-*a*]pyrazine (**6**). Reactions and conditions: (i) RMgX·LiCl (**23**, 1.2 equiv.), THF, 40 °C, 10 min; (ii) aq. workup or E-X (1.2 equiv.), THF, 25 °C, 2 h; (iii) DDQ (1.2 equiv.), THF, 25 °C, 16 h.

In addition, based on previously described nucleophilic addition reactions to pyrazolo[1,5-*a*]pyrimidine (**1**, Scheme 1)[4c] we have examined the addition of Grignard reagents triggered by a coordination at the most basic nitrogen N1 (see **24**). Thus, we have treated 6-chloroimidazo[1,2-*a*]pyrazine (**6**) with various organomagnesium halides complexed with lithium chloride of type **23**[28] (Scheme 8). Indeed, the reaction of **6** with 4-methoxyphenylmagnesium bromide·lithium chloride (**23a**)[28a] gave an intermediate magnesium species **25** which after water quenching provided dihydroimidazo[1,2-*a*]pyrazine **26a** in 63% yield. Due to instability of such partially saturated heterocycles, these compounds of type **26** were, after an aqueous work-up, directly oxidized with DDQ (DDQ = 2,3-dichloro-5,6-dicyano-1,4-benzoquinone), furnishing 8-arylated imidazo[1,2-*a*]pyrazines **27a–c** in 37–78% yield. This reaction sequence was also extended to the addition of alkylmagnesium reagents such as **23d-e** resulting in the alkylated N-heterocycles **27d-e** in 67–95% yield. Trapping of **25a** with $PhSO_2SPh$ followed by rearomatization with DDQ gave disubstituted imidazo[1,2-*a*]pyrazine **27f** in 33% isolated yield.

Conclusions

In summary, with the help of theoretical calculations such as pK_a determinations, N-basicity evaluations, and thermochemical analysis of the various Zn or Mg organometallic intermediates, we were able to fully rationalize the observed metalation selectivities of the underexplored fused N-heterocycle scaffold **6**. Despite the general usefulness of pK_a values and N-basicities, we find the relative stabilities of the Zn- or Mg-intermediates

 © 2023 The Author(s). Published by the Royal Society of Chemistry

Open Access Article. Published on 28 September 2023. Downloaded on 10/30/2025 1:26:33 AM. This article is licensed under a Creative Commons Attribution-NonCommercial 3.0 Unported Licence.

were key be more helpful for the rationalization of experimental results. In addition, we found that the coordination of additives such as LiCl to the N1 position were crucial for directing the metalation to the C2 or C8 positions due to stabilizing chelating interactions as shown for intermediate **17** in Scheme 6. This "chelate"-effect is equally possible in zinc intermediate **15** (Scheme 5).[11] We have successively metalated all positions of the 5,6-fused bicyclic N-heterocycle 6-chloroimidazo[1,2-*a*]pyrazine (**6**) using a combination of different bases such as TMPMgCl·LiCl (**11**) and/or $TMP_2Zn \cdot 2MgCl_2 \cdot 2LiCl$ (**12**) as well as TMPLi (**19**). The resulting metalated species were then quenched with different electrophiles giving access to a broad scope of functionalized imidazopyrazine derivatives. Furthermore, 6-chloroimidazo[1,2-*a*]pyrazine (**6**) underwent Pd-catalyzed cross-couplings using aryl, alkyl and benzylic zinc reagents allowing further functionalizations of this important heterocycle and a nucleophilic addition of Grignard reagents was also possible giving an access to partially saturated heterocycle (**26a**) with favorable solubilities. This calculation-assisted functionalization of heterocyclic scaffolds should be applicable to further uncommon heterocycles of pharmaceutical (or agrochemical) interest and deserve further exploration.

Data availability

Crystallographic data for compounds **7a**, **8b**, **16a** and **18a** has been deposited at the CCDC under 2258909–2258912. The datasets supporting this article have been uploaded as part of the ESI.†

Author contributions

A. K., A. K., A. S., Y. C. G. and S. K. R. performed and analyzed the experiments. K. K. measured and analyzed X-ray crystal structures. V. K. and H. Z. performed DFT calculations. A. K., A. K. and P. K. designed the experiments. A. K., H. Z. and P. K. prepared the manuscript with contributions of all authors.

Conflicts of interest

There are no conflicts to declare.

Acknowledgements

We thank the LMU Munich and the DFG for financial support. We thank Albemarle (Hoechst, Germany) for the generous gift of chemicals.

Notes and references

1 (*a*) R. D. Taylor, M. MacCoss and A. D. G. Lawson, *J. Med. Chem.*, 2014, **57**, 5845–5859; (*b*) E. Vitaku, D. T. Smith and J. T. Njardarson, *J. Med. Chem.*, 2014, **57**, 10257–10274; (*c*) D. C. Blakemore, L. Castro, I. Churcher, D. C. Rees, A. W. Thomas, D. M. Wilson and A. Wood, *Nat. Chem.*, 2018, **10**, 383–394.

2 (*a*) E. J. Corey, B. Czakó and L. Kürti, *Molecules and Medicine*, John Wiley & Sons, Hoboken, 2007; (*b*) l. D. Quin and J. A. Tyrell, *Fundamentals of Heterocyclic Chemistry: Importance in Nature and in the Synthesis of Pharmaceuticals*, John Wiley & Sons, Hoboken, 2010; (*c*) L. Guillemard, N. Kaplaneris, L. Ackermann and M. J. Johansson, *Nat. Rev. Chem.*, 2021, **5**, 522–545.

3 W. R. Pitt, D. M. Parry, B. G. Perry and C. R. Groom, *J. Med. Chem.*, 2009, **52**, 2952–2963.

4 (*a*) K. Snégaroff, T. T. Nguyen, N. Marquise, Y. S. Halauko, P. J. Harford, T. Roisnell, V. E. Matulis, O. A. Ivashkevich, F. Chevallier, A. E. H. Wheatley, P. C. Gros and F. Mongin, *Chem.–Eur. J.*, 2011, **17**, 13284–13297; (*b*) M. Balkenhohl, H. Jangra, I. S. Makarov, S.-M. Yang, H. Zipse and P. Knochel, *Angew. Chem. Int. Ed.*, 2020, **59**, 14992–14999; *Angew. Chem.*, 2020, **132**, 15102–15109; (*c*) S. K. Rout, A. Kastrati, H. Jangra, K. Schwärzer, A. S. Sunagatullina, M. Garny, F. Lima, C. Brocklehurst, K. Karaghiosoff, H. Zipse and P. Knochel, *Chem.–Eur. J.*, 2022, **28**, e202200733.

5 K.-i. Kusakabe, N. Ide, Y. Daigo, T. Itoh, T. Yamamoto, H. Hashizume, K. Nozu, H. Yoshida, G. Tadano, S. Tagashira, K. Higashino, Y. Okano, Y. Sato, M. Inoue, M. Iguchi, T. Kanazawa, Y. Ishioka, K. Dohi, Y. Kido, S. Sakamoto, S. Ando, M. Maeda, M. Higaki, Y. Baba and Y. Nakamura, *J. Med. Chem.*, 2015, **58**, 1760–1775.

6 J. G. Kettle, S. Brown, C. Crafter, B. R. Davies, P. Dudley, G. Fairley, P. Faulder, S. Fillery, H. Greenwood, J. Hawkins, M. James, K. Johnson, C. D. Lane, M. Pass, J. H. Pink, H. Plant and S. C. Cosulich, *J. Med. Chem.*, 2012, **55**, 1261–1273.

7 (*a*) R. C. X. Brys, P. Edwards, W. Schmidt, M. J. I. Andrews, M. S. Chambers, J. A. Clase, V. Birault, K. L. Hirst, A. Macleod, G. Bar, C. J. Harris and P. Huxley, WIPO (PCT), WO2007131991A1, 2007; (*b*) T. Yu, D. B. Belanger, A. D. Kerekes, Z. Meng, J. R. Tagat, S. J. Esposite, A. K. Mandal, Y. Xiao, B. A. Kulkarni, Y. Zhang, P. J. Curran, R. Doll and M. A. Siddiqui, WIPO (PCT), WO2008156614A2, 2008; (*c*) M. Koppitz, U. Klar, R. Jautelat, D. Kosemund, R. Bohlmann, B. Bader and P. Lienau, WIPO (PCT), WO2012080229A1, 2011.

8 Y. Jin, P. Bu, Q. He, J. Lan, F. Zhou, L. Zhang and X. He, WIPO (PCT), WO2016050165, 2016.

9 (*a*) I. Hyodo, M. Tobisu and N. Chatani, *Chem.–Asian J.*, 2012, **7**, 1357–1365; (*b*) S. K. Guchhait, S. Kandekar, M. Kashyap, N. Taxak and P. V. Bharatam, *J. Org. Chem.*, 2012, **77**, 8321–8328; (*c*) V. Gembus, J.-F. Bonfanti, O. Querolle, P. Jubault and C. Hoarau, *Org. Lett.*, 2012, **14**, 6012–6015; (*d*) B. M. Jonson and M. P. Huestis, *Eur. J. Org Chem.*, 2014, 1589–1593; (*e*) B. Zhang, W. Zhang, J. Wang, Q. Wang, N. Kambe and R. Qiu, *Org. Lett.*, 2022, **24**, 7918–7923.

10 (*a*) B. Haag, M. Mosrin, I. Hiriyakkanavar, V. Malakhov and P. Knochel, *Angew. Chem. Int. Ed.*, 2011, **50**, 9794–9824; *Angew. Chem.*, 2011, **123**, 9968–9999; (*b*) A. Kremsmair, J. H. Harenberg, K. Schwärzer, A. Hess and P. Knochel, *Chem. Sci.*, 2021, **12**, 6011–6019; (*c*) A. Kremsmair, A. Hess,

Open Access Article. Published on 28 September 2023. Downloaded on 10/30/2025 1:26:33 AM. This article is licensed under a Creative Commons Attribution-NonCommercial 3.0 Unported Licence.

B. Heinz and P. Knochel, *Chem.–Eur. J.*, 2022, **28**, e202103269.

11 For further information, see ESI.†.

12 (*a*) K. Reddy, G. Martinez Botella, A. M. Griffin and E. Brian, Praxis Precision Medicines, Inc., WO2018098500A1, 2018; (*b*) S. B. Hoyt, C. J. Thomas, D. T. Starczynowski, J. S. Rosenbaum and G. Gracia Maldonado, Kurome Therapeutics Inc., WO2022140647A1, 2022.

13 W. C. Lumma Jr., W. C. Randall, E. L. Cresson, J. R. Huff, R. D. Hartman and T. F. Lyon, *J. Med. Chem.*, 1983, **26**, 357–363.

14 (*a*) A. Krasovskiy, V. Krasovskaya and P. Knochel, *Angew. Chem. Int. Ed.*, 2006, **45**, 2958–2961; *Angew. Chem.*, 2006, **118**, 3024–3027; (*b*) G. C. Clososki, C. J. Rohbogner and P. Knochel, *Angew. Chem. Int. Ed.*, 2007, **46**, 7681–7684; *Angew. Chem.*, 2007, **119**, 7825–7828; (*c*) A. Hess, A. Kremsmair and P. Knochel, *Encyclopedia of Reagents for Organic Synthesis*, Wiley VCH, 2021, DOI: **10.1002/047084289X.rn02373**.

15 (*a*) S. H. Wunderlich and P. Knochel, *Angew. Chem. Int. Ed.*, 2007, **46**, 7685–7688; *Angew. Chem.*, 2007, **119**, 7829–7832; (*b*) M. Mosrin and P. Knochel, *Org. Lett.*, 2009, **11**, 1837–1840; (*c*) T. Klatt, P. Knochel and M. Mosrin, *Encyclopedia of Reagents for Organic Synthesis*, Wiley VCH, 2015, DOI: **10.1002/047084289X.rn01806**.

16 (*a*) A. Hess, J. P. Prohaska, S. B. Doerrich, F. Trauner, F. H. Lutter, S. Lemaire, S. Wagschal, K. Karaghiosoff and P. Knochel, *Chem. Sci.*, 2021, **12**, 8424–8429; (*b*) A. Kremsmair, S. Graßl, C. J. B. Seifert, E. Godineau and P. Knochel, *Synthesis*, 2021, **53**, 4068–4074; (*c*) A. S. Sunagatullina, F. H. Lutter and P. Knochel, *Angew. Chem. Int. Ed.*, 2022, **61**, e202116625; *Angew. Chem.*, 2022, **134**, e202116625; (*d*) A. Kremsmair, A. S. Sunagatullina, L. J. Bole, P. Mastropierro, S. Graßl, H. R. Wilke, E. Godineau, E. Hevia and P. Knochel, *Angew. Chem. Int. Ed.*, 2022, **61**, e202210491; *Angew. Chem.*, 2022, **134**, e202210491.

17 No organometallic intermediates have been isolated or characterized. Their structures are reasonable based on the obtained products and precedent in the literature as found in ref. 10.

18 Other regioisomers are, if any, formed in negligible amounts (less than 2%). However, these functionalized heterocycles show moderate solubility, which may be at least partly responsible for low overall yields.

19 P. Knochel, M. C. P. Yeh, S. C. Berk and J. Talbert, *J. Org. Chem.*, 1988, **53**, 2390–2392.

20 K. Fujiki, N. Tanifuji, Y. Sasaki and T. Yokoyama, *Synthesis*, 2002, 343–348.

21 E.-i. Negishi, *Angew. Chem. Int. Ed*, 2011, **50**, 6738–6764; *Angew. Chem.*, 2011, **123**, 6870–6897.

22 Deprotonation at position 5 requires higher temperature because a weaker base such as TMP2Zn·2MgCl2·LiCl is used compared to a stronger TMPMgCl·LiCl base capable of deprotonation at lower temperature. In addition, intermediates generated when using TMPZn-bases are usually more stable at elevated temperature.

23 M. C. Whisler, S. MacNeil, V. Snieckus and P. Beak, *Angew. Chem. Int. Ed*, 2004, **43**, 2206–2225; *Angew. Chem.*, 2004, **116**, 2256–3227.

24 Quenching with other electrophiles such as an aldehyde led to only traces of isolated product.

25 (*a*) A. Krasovskiy and P. Knochel, *Angew. Chem. Int. Ed.*, 2004, **43**, 3333–3336; *Angew. Chem.*, 2004, **116**, 3396–3399; (*b*) A. Metzger, F. M. Piller and P. Knochel, *Chem. Commun.*, 2008, 5824–5826; (*c*) V. Dhayalan and P. Knochel, *Synthesis*, 2015, 3246–3256; (*d*) F. H. Lutter, L. Grokenberger, P. Spieß, J. M. Hammann, K. Karaghiosoff and P. Knochel, *Angew. Chem. Int. Ed.*, 2020, **59**, 5546–5550; *Angew. Chem.*, 2020, **132**, 5591–5595.

26 M. G. Organ, S. Avola, I. Dubovyk, N. Hadei, E. A. B. Kantchev, C. J. O'Brien and C. Valente, *Chem.–Eur. J.*, 2006, **12**, 4749–4755.

27 (*a*) M. G. Organ, S. Calimsiz, M. Sayah, K. H. Hoi and A. J. Lough, *Angew. Chem. Int. Ed.*, 2009, **48**, 2383–2387; *Angew. Chem.*, 2009, **121**, 2419–2423; (*b*) J. Skotnitzki, A. Kremsmair, D. Keefer, Y. Gong, R. de Vivie-Riedle and P. Knochel, *Angew. Chem. Int. Ed.*, 2020, **59**, 320–324; *Angew. Chem.*, 2020, **132**, 328–332.

28 (*a*) A. Kremsmair, H. R. Wilke, M. M. Simon, Q. Schmidt, K. Karaghiosoff and P. Knochel, *Chem. Sci.*, 2022, **13**, 44–49; (*b*) A. Kremsmair, H. R. Wilke, J. H. Harenberg, B. R. G. Bissinger, M. M. Simon, N. Alandini and P. Knochel, *Angew. Chem. Int. Ed.*, 2023, **62**, e202214377; *Angew. Chem.*, 2023, **135**, e202214377.

 © 2023 The Author(s). Published by the Royal Society of Chemistry